Applied Thermal Engineering 76 (2015) 220–232

Contents lists available at ScienceDirect

Applied Thermal Engineering

journal homepage: www.elsevier.com/locate/apthermeng

Research paper

A numerical study on the turbulent heat transfer enhancement of Rodbaffle heat exchanger with staggered tubes supported by round rods with arc cuts

Yonghua You [a, b, *], Fahui Zhang [a], Aiwu Fan [c], Fangqin Dai [a, b], Xiaobing Luo [c], Wei Liu [c]

[a] State Key Lab. of Refractory and Metallurgy, Wuhan University of Science and Technology, Wuhan 430081, China
[b] Key Laboratory for Ferrous Metallurgy and Resources Utilization of Ministry of Education, Wuhan University of Science and Technology, Wuhan 430081, China
[c] School of Energy and Power Engineering, Huazhong University of Science and Technology, Wuhan 430074, China

HIGHLIGHTS

- Staggered alignment is studied to raise performances of Rodbaffle heat exchangers.
- Effects of baffle distance, rod diameter, etc., are studied with numerical method.
- Combined parameters (hA) of heat exchangers rise by ~64% with current supports.
- Overall thermo-hydraulic performances lie in the range of 821–6243 W/(m K kPa).

ARTICLE INFO

Article history:
Received 9 July 2014
Accepted 17 November 2014
Available online 27 November 2014

Keywords:
Numerical study
Turbulent heat transfer
Rodbaffle heat exchanger
Staggered alignment
Rod with arc cuts

ABSTRACT

To improve the shellside thermo-hydraulic performance of Rodbaffle heat exchangers, round rods with arc cuts are used to support staggered tubes in the current investigation, and numerical computation on the turbulent heat transfer enhancement is conducted. Comparisons between staggered and non-staggered alignments are performed. Meanwhile, the influences of baffle distance (L_b), rod diameter (d) and clamping method of tubes are investigated. Computation results demonstrate that convection heat transfer coefficient (h) and combined parameter (hA) of staggered tubes clamped with the method of one tube within two rods (OTWTR) are about 41.9% and 63.8% larger than the counterparts of non-staggered ones, respectively, while the pressure loss is doubled. Moreover, it is observed that similar to the pressure drop (β), h of staggered alignment, ranging between 2835 and 10,825 W/(m^2 K), increases with a decreasing L_b or a rising d. The overall thermo-hydraulic performance, h/β, varies from 821 to 6243 W/(m K kPa), and a larger L_b, or a smaller d facilitates a larger h/β. In addition, the clamping method of one tube by one rod is found to generate a much smaller β and thus a larger h/β compared with the counterparts of OTWTR or non-staggered alignment. Finally, streamtraces and contours are presented for discussions.

1. Introduction

Shell-and-tube heat exchangers (STHXs) are widely applied in various industrial fields such as petroleum refining, power generation and chemical process, etc. It is well known that the traditional STHXs make use of segmented baffles to induce fluid flowing across tube bundles to enhance the heat transfer rate on the shellside. However, the shellside zigzag flow results in a large flow resistance and vibration level, as well as large-scale recirculation "dead" regions [1,2]. To solve these problems and improve the overall performance of traditional STHXs, in addition to developing a variety of high efficient tubes and tube inserts [3–5], scholars and engineers have put forward and investigated many new types of tube supports, such as orifice baffle [6,7], helical baffle [8–10], ring support [11] and flower baffle [12,13], etc. These tube supports induce fluid flowing longitudinally or helically on the shellside, thus the pressure loss and vibration level are substantially decreased. Meanwhile, the recirculation region (and thus back mixing of working fluid) is small with such baffles, which favors the reinforcement of shellside heat transfer rates.

* Corresponding author. State Key Lab. of Refractory and Metallurgy, Wuhan University of Science and Technology, 947 Heping Road, Wuhan 430081, China. Tel.: +86 027 68862168.
E-mail address: hust_yyh@163.com (Y. You).

http://dx.doi.org/10.1016/j.applthermaleng.2014.11.048
1359-4311/

Rodbaffle supports, initially put forward and developed by Phillips Petroleum Company to eliminate flow-induced tube vibrations of segmental baffle STHXs, are another type of widely-applied tube supports with longitudinal flow patterns [14–16]. These tube supports have small pressure drops and good overall thermo-hydraulic performances, and thus are widely investigated with both numerical and experimental methods. To name a few, X. Deng and S. Deng [11] investigated the turbulent heat transfer enhancement of roughened tube bundles supported by rods, and analyzed the physical mechanism by measuring fluid velocity and turbulence distributions with LDV. Dong et al. conducted the numerical and experimental investigations in the shellside thermal augmentation of Rodbaffle heat exchangers [17]. They built the simplified model of unit channel, and computed with the software of FLUENT. Their numerical results agree with experimental data well. Ma et al. studied the influence of rod profiles on shellside thermo-hydraulic performances with the commercial CFD software [18]. It is found that elliptical rods generate the best overall performances, while the square ones result in the largest Nu number.

As far as we know, Rodbaffle heat exchangers usually arrange the tubes in the non-staggered alignment, and the above investigations of Rodbaffle are all based on the non-staggered tubes. However, the non-staggered alignment is a loose arrangement, and the heat transfer rate needs more enhancements. To crack the nut, some solutions were put forward and investigated. Liu et al. [19] proposed to arrange spoilers between every four adjacent tubes. Dong et al. used two kinds of tubes with different diameters in the same Rodbaffle heat exchanger to increase the heat transfer surface [20]. However, the above improvements are limited.

As is well known, the staggered alignment of tubes facilitates a better shellside thermal augmentation compared with the corresponding non-staggered one, because it increases heat transfer area and the fluid is more intensively disturbed. However, up to now, the investigation in the thermal augmentation of staggered tubes supported by rods is relatively limited. Yan et al. used curved rods to support staggered tubes and conducted the experimental investigation. Experimental data demonstrated that both the heat transfer rate and flow resistance are superior to the counterparts of segmental baffles [21]. It is noted that the shell diameter of heat exchanger is small, and the effects of geometrical parameters are not investigated.

In the present paper, straight round rods with arc cuts are proposed to be welded with rings as new tube supports, and they are alternately arranged to fix tubes in the staggered alignment, as depicted in Fig. 1. Numerical computations on the shellside turbulent heat transfer are performed for the new type of tube supports, and comparisons of thermo-hydraulic performances with those of non-staggered alignment are conducted. Moreover, the influences of several geometrical factors, i.e., baffle distance, rod diameter and clamping methods of tubes, are investigated. In addition, the contours of velocity, temperature and pressure, as well as the fluid streamtraces, are presented for the discussions.

2. Geometrical models

Fig. 1 depicts the baffle rings welded with straight round rods for the arrangement of tubes in the staggered alignment. The adjacent baffle rings are installed with a phase difference of (+/−) 60° and the intersections with tubes are cut off. Tubes are fixed by rods with two methods, i.e., one tube within two rods (OTWTR) and one tube by one rod (OTBOR) [15], which are depicted in Fig. 1(a) and (b), respectively.

In the current investigation, the diameter of tube, characterized by D, equals to 25 mm, and d stands for the rod diameter, taking the values of 6, 7, 8 and 9 mm. The tube pitch, s, is equal to 32 mm, while the Rodbaffle distance (L_b) varies from 120 to 240 mm with a constant step of 30 mm.

3. Numerical model and computational scheme

3.1. Governing equations

Water is selected as the shellside working fluid. It is treated as a Newtonian, incompressible fluid with constant physical properties, since the temperature difference between fluid and tube wall is limited in the current computation. Moreover, it is assumed that the flow is stable and turbulent. The viscous heating and pressure power are neglected due to the limited fluid velocity and incompressible medium assumption.

Based on the above assumptions, the conservation equations of continuity, momentum and energy for the turbulent heat transfer of fluid flowing on the shellside are presented in the tensor form as following [17,22,23]:

Continuity equation:

$$\frac{\partial(\rho u_j)}{\partial x_j} = 0 \tag{1}$$

Momentum equation:

$$\frac{\partial(\rho u_i u_j)}{\partial x_j} = -\frac{\partial p}{\partial x_i} + \frac{\partial}{\partial x_j}\left(\mu_{\text{eff}}\left(\frac{\partial u_i}{\partial x_j} + \frac{\partial u_j}{\partial x_i}\right)\right) \tag{2}$$

Energy equation:

$$\frac{\partial(\rho c_p T u_j)}{\partial x_j} = \frac{\partial}{\partial x_j}\left(\lambda_{\text{eff}}\left(\frac{\partial T}{\partial x_j}\right)\right) \tag{3}$$

where T and p stand for fluid temperature and pressure, respectively; u is the fluid velocity; ρ and c_p are fluid density and constant-pressure specific heat, respectively. μ_{eff} stands for effective dynamic viscosity, equal to the sum of laminar and turbulent dynamic viscosities, i.e., $\mu_{\text{eff}} = \mu_l + \mu_t$. The effective thermal conductivity, λ_{eff}, is calculated by $\lambda_{\text{eff}} = \lambda_l + \mu_t c_p/\text{Pr}_t$, where λ_l and Pr_t are the laminar conductivity and turbulent Prandtl number, respectively.

Standard k–ε turbulence model together with standard wall function is adopted for the current computation [17,18]. The conservation equations of turbulent kinetic energy and its dissipation rate are given below:

For turbulence kinetic energy k:

$$\frac{\partial(\rho k u_j)}{\partial x_j} = \frac{\partial}{\partial x_j}\left(\left(\mu_l + \frac{\mu_t}{\sigma_k}\right)\frac{\partial k}{\partial x_j}\right) + G_k - \rho\varepsilon \tag{4}$$

For turbulence kinetic energy dissipation rate ε:

$$\frac{\partial(\rho \varepsilon u_j)}{\partial x_j} = \frac{\partial}{\partial x_j}\left(\left(\mu_l + \frac{\mu_t}{\sigma_\varepsilon}\right)\frac{\partial \varepsilon}{\partial x_j}\right) + \frac{C_{1\varepsilon}\varepsilon}{k}G_k - C_{2\varepsilon}\rho\frac{\varepsilon^2}{k} \tag{5}$$

where $\mu_t = \rho C_\mu k^2/\varepsilon$; $G_k = 2\mu_t E_{ij} E_{ij}$; $E_{ij} = 1/2((\partial u_i/\partial x_j) + (\partial u_i/\partial x_j))$.

The constants for the current turbulent model are set as below [24]:

$$C_\mu = 0.09;\ \ C_{1\varepsilon} = 1.44;\ \ C_{2\varepsilon} = 1.92;\ \ \sigma_k = 1.0;\ \ \sigma_\varepsilon = 1.3$$

3.2. Computation region, mesh and boundary conditions

For an STHX with hundred of tubes and dozens of baffles, considerable computer resources are required to compute the whole shellside flow field. On the other hand, the influence of shell wall on the shellside thermo-hydraulic performance is limited in such a heat exchanger, and it is economic and efficient to compute

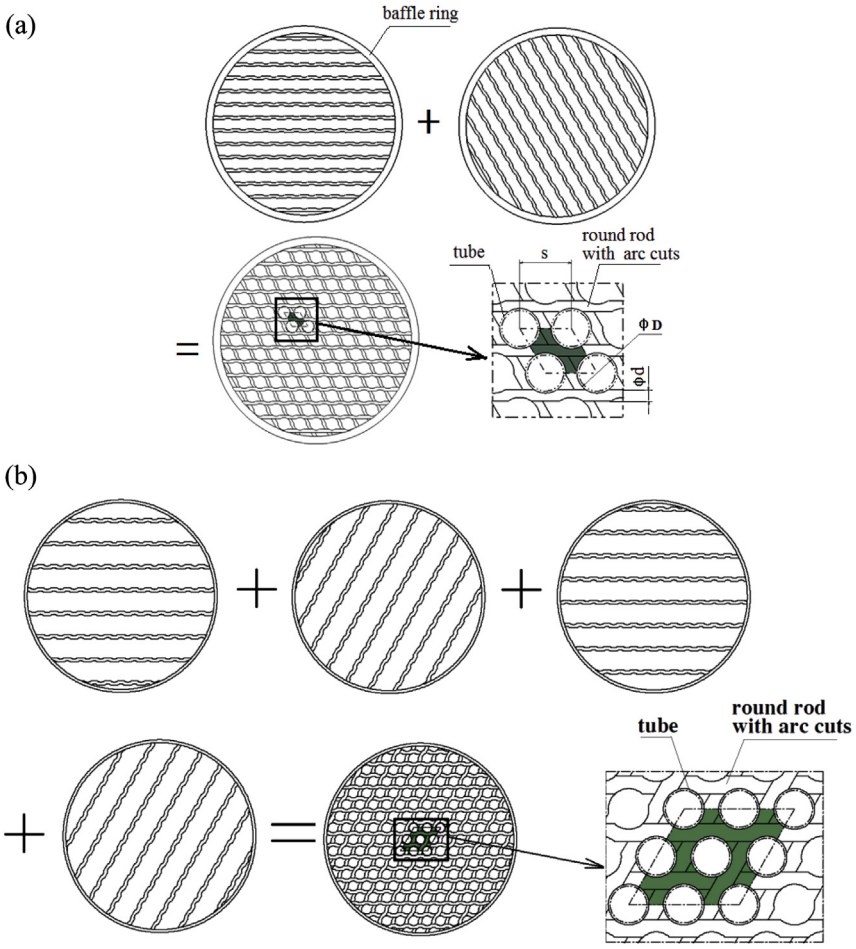

Fig. 1. Assembly schematic of baffle rings welded with round rods for arranging staggered tubes, where hatched region is adopted as the unit channel. (a) For the clamping method of one tube within two rods (OTWTR); (b) for the clamping method of one tube by one rod (OTBOR).

one unit channel for the whole shellside performance [7,17–19]. In the current numerical study, two unit channels, i.e., the shade zones in Fig. 1(a) and (b), are made out based on the assumptions of fully-developed flow and periodic flow patterns for the cases of one tube within two rods (OTWTR) and one tube by one rod (OTBOR), respectively. Two times and four times baffle distances are set as the longitudinal length of computation domains of the two clamping methods, respectively.

Gambit 2.4 is used for geometrical modeling and mesh generation. Hybrid meshes are adopted, i.e., tetrahedron grid in the region near rod and hexahedral cell for the rest, as showed in Fig. 2(a) and (c) (for OTWTR and OTBOR, respectively). Momentum boundaries of all solid walls are of no slip and no penetration, and constant temperature and zero heat flux are specified for tube and rod wall, respectively. The inlet and outlet, as well as the interface planes with adjacent fluid, i.e., p1, p1′ and p2, p2′ in Fig. 2, are set as periodic boundary conditions, and mass flow rate along the tube axis is specified for the computation.

The shellside fluid velocity varies periodically in the fully-developed region, while the pressure doesn't have such a feature. For this purpose, a transform is conducted on pressure by introduce an intermediate variable of pressure [24], i.e.,

$$\widehat{p} = p(x,y,z=0) + \beta z \tag{6}$$

where β refers to the averaged longitudinal pressure gradient and here z is the direction of bulk flow. As for the case of OTWTR, $\beta = p(x,y,z) - p(x,y,z+2L_b)/2L_b$.

It is clear that similar to fluid velocity u, $\widehat{p}$ varies periodically in the fully-developed region.

3.3. Computational scheme and validation

The computational scheme is similar to that applied in our previous study [7]. One unit channel applied with periodic boundary is computed, and the mass flow rate is set in accordance with the desired Re number. The velocity and temperature distributions at the periodic boundaries, as well as the pressure gradient, are computed by iteration.

Three dimensional double-precision version of Fluent 14.0 is adopted as the solver. All above-mentioned equations accompanied by boundary conditions are discretized with finite volume formulation. The pressure term is treated with standard scheme, while the momentum, energy, turbulence kinetic energy and its dissipation rate are treated with the second-order upwind scheme. Numerical computations are conducted with pressure-based solver. Pressure and velocity are coupled with the 'SIMPLE' algorithm. All equations take the convergent criterions of relative residual of 1E-4 except energy taking 1E-8. In addition, the wall y plus is evaluated after the convergence to guarantee the requirement of standard wall function is met. In more details, wall $y+$ lies in the range between ~20 and 100 in the current computation. The mesh independence is checked on one typical case of OTWTR. Three sets of grids (about 60 k, 120 k and 160 k) are computed, the relative deviations of averaged convection heat transfer coefficient and

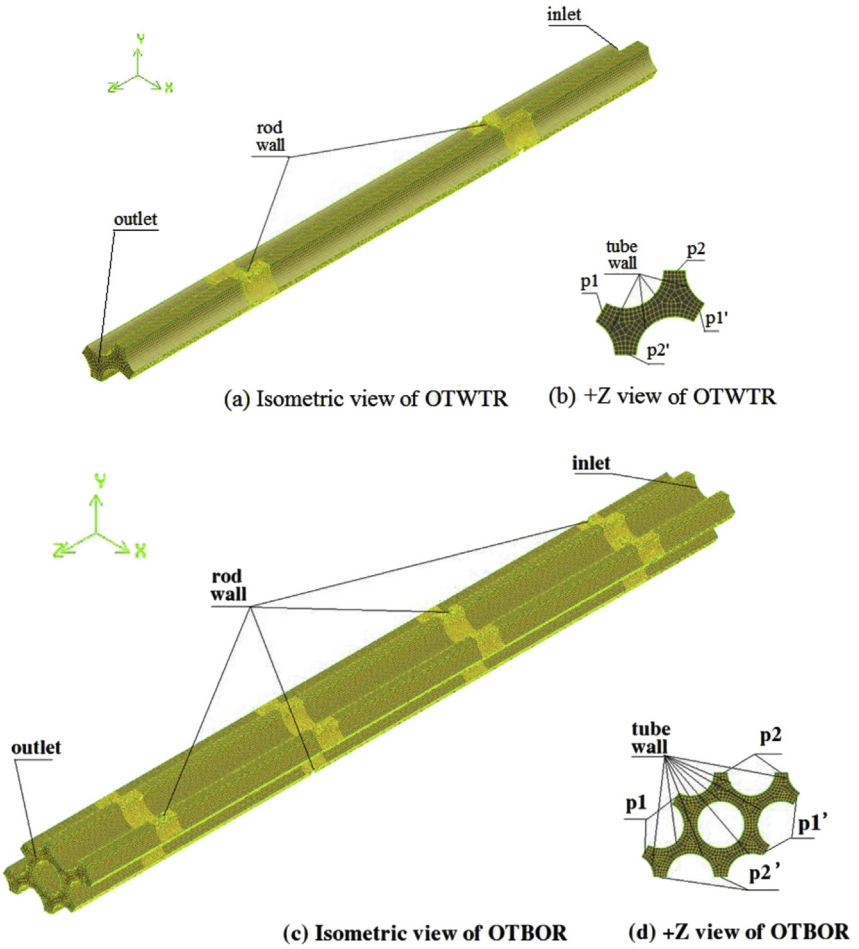

Fig. 2. Computation domain and mesh generation for fluid flowing longitudinally in staggered tubes supported with rods. (a) and (b) for the clamping method of one tube within two rods (OTWTR), while (c) and (d) for the method of one tube by one rod (OTBOR).

longitudinal pressure gradient between the last two sets of meshes are within 3%. Thus the second set of mesh is adopted for the final computation.

To validate the present numerical model, non-staggered tubes with round rods are computed and compared with empirical data. Different turbulent models of eddy viscosity are compared, and standard $k-\varepsilon$ is found to behave well from the viewpoints of precision and convergences, i.e., the computed Nu numbers conform to the empirical relation of Eq. (7) [17] with the relative deviation within 7.5%, as depicted in see Fig. 3.

$$\mathrm{Nu} = 0.0589\mathrm{Re}^{0.815}\mathrm{Pr}^{1/3}\left(\frac{L_b}{D_h}\right)^{-0.303}\left(\frac{\mu_w}{\mu_f}\right)^{0.14} \tag{7}$$

where D_h refers to the characteristic dimension, calculated by Eq. (9).

It is noted that the correlation of Eq. (7) has been verified with a good precision in the Re range between 2000 and 15,000 by the comparison with that of Phillips Petroleum Corporation [17].

Moreover, the computed pressure loss by the unit channel model is also compared with the empirical data of Phillips Petroleum Corporation [17]. Since the viscosity of water used in current computation is different from that of [17] (1.004E-3–8.015E-4 kg/(m s)), a multiplier of 1.058 (equal to the quarter power of viscosity ratio) is used, and the maximum relative deviation is about 7% based on same fluid velocities.

In addition, the full section model is constructed to compute the shellside turbulent heat transfer for a Rodbaffle heat exchanger with staggered tubes, and the computed velocity contour, together with pressure loss and convection heat transfer rate, are compared

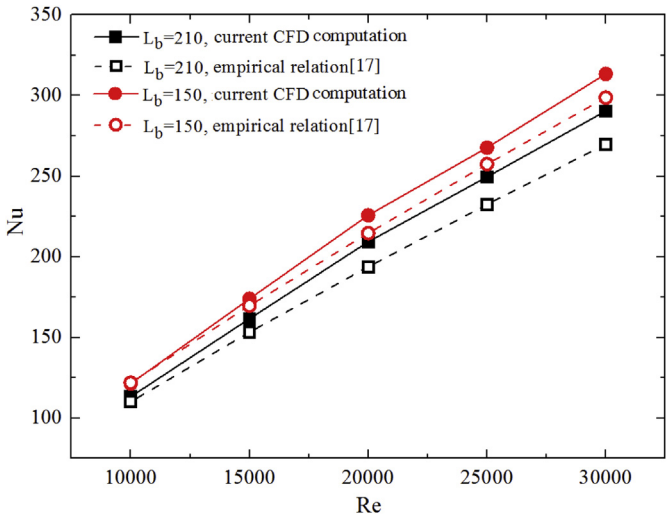

Fig. 3. Comparison of Nu number between current CFD computation and empirical relation for a Rodbaffle heat exchanger with non-staggered tubes.

with the counterparts obtained by unit channel model, as depicted in Fig. 4(a)–(c). It is noted that because the shell diameter is limited and tube number is small, the assumption of same averaged fluid velocities between rods is made to determine the mass flow rate of unit channel model, and the averaged convection heat transfer coefficient of central seven tubes in full section model are used for the comparison. From Fig. 4(a) and (b), it is seen that the velocity contour of unit channel model has a large resemblance with the counterpart of full section model, and their magnitudes of fluid velocity are very close. The curves of pressure loss and convection heat transfer coefficient (see Fig. 4(c)) obtained by the two types of models have same variation trends, and the relative deviations are equal to about 6.3% and 3.5%, respectively.

From the above comparisons, it can be said that the current numerical computation is reliable and has a reasonable precision.

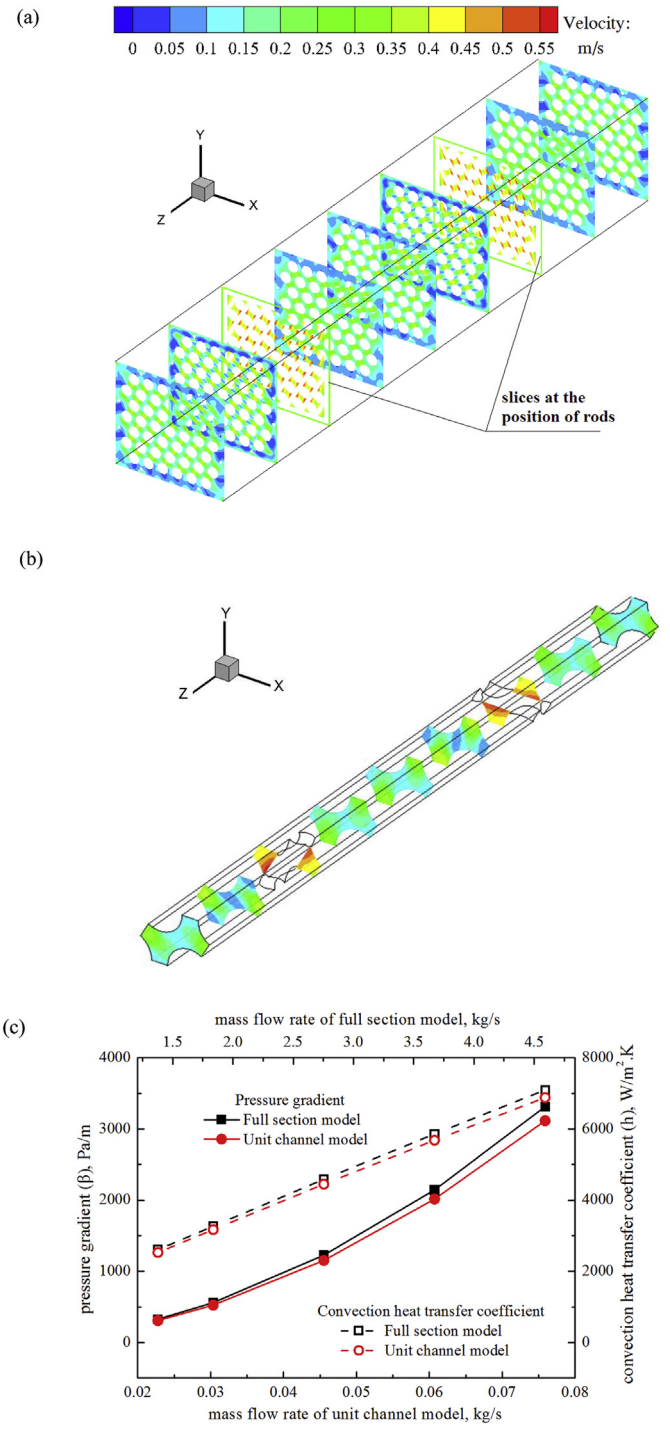

Fig. 4. Comparisons of velocity contour and curves of pressure loss and convection heat transfer coefficient between full section model and unit channel model for a Rodbaffle shell-and-tube heat exchanger of rectangular section installed with staggered tubes. (a) Contour of velocity magnitude on the shellside predicted by full section model, in which the longitudinal length is magnified by 4 times for distinction; (b) contour of velocity magnitude on the shellside predicted by unit channel model; (c) comparison of pressure loss and convection heat transfer coefficient between full section model and unit channel model.

3.4. Calculation methods of thermo-hydraulic performances

3.4.1. Re number and characteristic dimension

Re number of longitudinal flow between tubes supported by rods is defined as

$$\mathrm{Re} = \rho u_{m,z} D_h / \mu_1 \tag{8}$$

where $u_{m,z}$ stands for the averaged longitudinal velocity magnitude at the section without baffles; D_h represents the characteristic dimension, calculated by Eqs. (9) and (10) for the non-staggered and staggered alignments [15,17], respectively.

$$D_h = \frac{4s^2 - \pi D^2}{\pi D} \tag{9}$$

$$D_h = \frac{2\sqrt{3s^2} - \pi D^2}{\pi D} \tag{10}$$

where D, s refer to the tube diameter and tube pitch, respectively.

3.4.2. Convection heat transfer coefficient and Nu number

The averaged convection heat transfer coefficient of tube walls, h, is calculated with the Newton' s law of cooling [25], i.e.,

$$h = q_w \Big/ \left(T_w - T_{f,m}\right) \tag{11}$$

where q_w and T_w stand for the area-weighted mean heat flux and temperature of tube wall, respectively; while $T_{f,m}$ represents the mass-weighted mean temperature of fluid [4].

Nusselt number, Nu, is calculated by

$$\mathrm{Nu} = \frac{hD_h}{\lambda_l} \tag{12}$$

3.4.3. Pressure drop and friction factor

Since the periodic boundary is adopted in the numerical computation, the solver of Fluent computes the pressure gradient (β) and intermediate variable of pressure ($\widehat{p}$) with the specified mass flow rate, and the real pressure is obtained by Eq. (6).

The average friction factor, f, is calculated by

$$f = \frac{2\beta D}{\rho u_{m,z}^2} \tag{13}$$

3.4.4. Overall thermo-hydraulic performance

In the current investigation, the ratio between convection heat transfer coefficient and pressure gradient [18], i.e., h/β, is adopted to evaluate the overall performance of heat transfer enhancement.

4. Results and discussions

4.1. Comparisons of thermo-hydraulic performances between non-staggered and staggered tubes supported with round rods

Two baffle distances, i.e., L_b = 150 and 210 mm, are adopted to compare the thermo-hydraulic performances of staggered tubes with the counterparts of non-staggered ones in the current investigation. It is noted that here staggered tubes are clamped with the method of one tube within two rods.

4.1.1. Comparison of heat transfer rate

Fig. 5(a) and (b) depicts the variations of Nu number and convection heat transfer coefficient (h) with Re number for non-staggered and staggered alignments of tubes in the turbulent flow regime, respectively. It can be seen that the two alignments have a larger Nu and h at a smaller baffle distance (L_b) condition, and the two parameters increase with the increment of Re number. Moreover, one can observe from Fig. 5(a) and (b) that, compared with non-staggered tubes supported by rods, the staggered alignment generates a larger Nu and h at the same Re. In more details, Nu is increased by about 1.9%–6.05%, while h has the increments of 38.9%–44.8%. In addition, compared with non-stagger alignment, staggered one accommodate more tubes, and thus more heat transfer area in the same shell. Therefore, the comprehensive parameter, i.e., hA, is put forward and compared between staggered and non-staggered alignments in the current investigation, as showed in Fig. 5(b) with the right vertical axis. With the comparison, it is found that the staggered alignment can increase heat flow by about 60.4%–67.2% with the same shell.

4.1.2. Comparison of pressure loss

The variations of pressure gradient (β) with Re number are depicted in Fig. 5(c) for non-staggered and staggered tubes supported by rods. It is seen that the two alignments have a larger β at a smaller baffle distance (L_b), and β increases with the increment of Re number. Moreover, one can observe from Fig. 5(c) that, staggered alignment generates a larger β than non-staggered alignment at the same Re. In more details, the pressure loss of staggered alignment is almost doubled.

4.1.3. Comparison of overall thermo-hydraulic performance

The variations of overall thermo-hydraulic performance (h/β) with Re number are depicted in Fig. 5(d) for non-staggered and staggered alignments. It can be seen that different with h or β, h/β has a larger value at a larger baffle distance (L_b), and it decreases with a rising Re number. The reason for the phenomena is that the increase of pressure drop is always quicker than that of convection heat transfer coefficient. Moreover, one can observe from Fig. 5(d) that the staggered alignment generates a smaller overall thermo-hydraulic performance than that of non-staggered alignment at the same Re condition. In more details, h/β is decreased by about 34%.

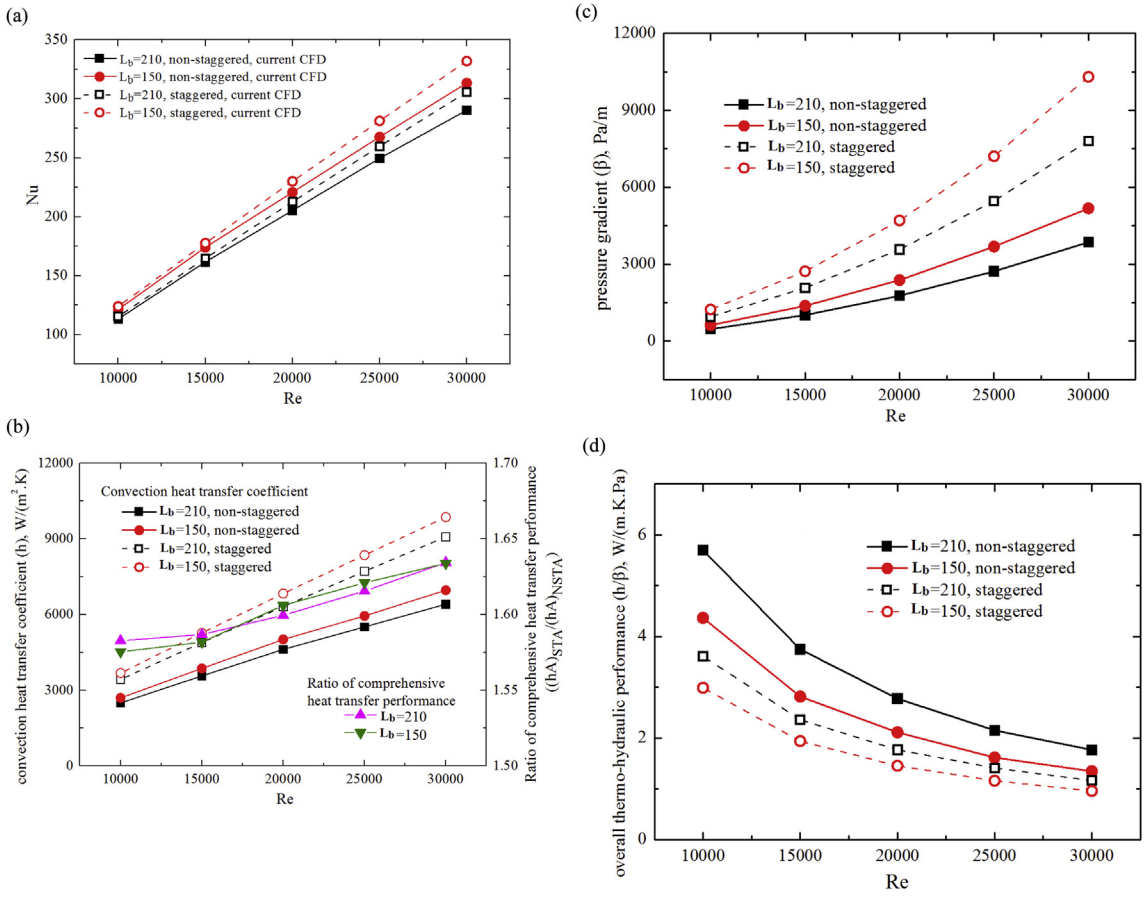

Fig. 5. Comparisons of thermo-hydraulic performances between non-staggered and staggered tubes under different Re conditions. Tubes are clamped with the method of one tube within two rods (OTWTR). (a) Comparison of Nu number; (b) comparisons of convection heat transfer coefficients and comprehensive heat transfer performance (i.e., the product of convection heat transfer coefficient and heat transfer area); (c) comparison of pressure loss; (d) comparison of overall thermo-hydraulic performances (i.e., the ratio between convection heat transfer coefficient and pressure gradient).

The above comparisons indicate that compared with non-staggered alignment, staggered alignment can considerably increase heat flow at the same shell. Despite the fact that staggered alignment can result in a substantial increment of pressure loss, it is still worthwhile because some industrial users may tolerate the increment of pumping power for a higher heat transfer coefficient.

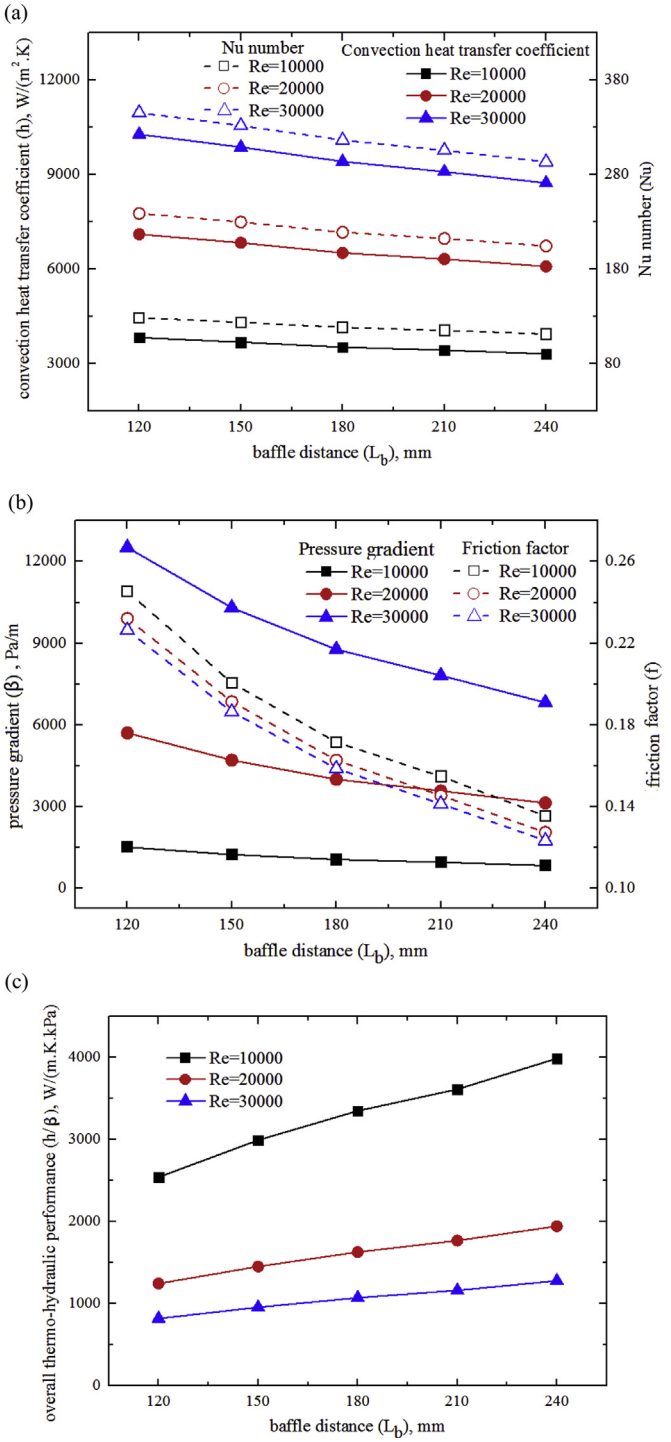

Fig. 6. Variations of thermo-hydraulic performances with baffle distance under different Re conditions. Tubes are clamped with the method of one tube within two rods (OTWTR). (a) Variations of convection heat transfer coefficient and Nu number; (b) variations of pressure loss and friction factor; (c) variation of overall thermo-hydraulic performance.

Therefore, in the current investigated, the effects of geometrical factors on thermo-hydraulic performances are studied for staggered tubes supported by the proposed round rods.

4.2. Variations of thermo-hydraulic performance with geometrical factors

4.2.1. Effects of baffle distance

Fig. 6(a) and (b) depicts the effects of baffle distance (L_b) on the shellside performances of heat transfer and flow resistance for staggered tubes clamped by current rods with the method of one tube within two rods (OTWTR), respectively, where three different Re numbers (i.e., Re = 10,000, 20,000 and 30,000) are computed. It is seen from Fig. 6(a) and (b) that the curves of different Re number have similar variation tendencies, and both convection heat transfer coefficient (h) and pressure gradient (β) increase with the decrement of L_b under the condition of same Re. For an instance, when L_b drops from 240 to 120 mm, the relative variations of the two parameters equal to 17% and 82.5% at Re = 20,000, respectively. In more details, h rises from 6092 to 7117 W/(m^2 K), while β increases from 3128 to 5705 Pa/m. Moreover, one can see in Fig. 6(a) and (b) that h and β increase with Re. When Re is increased from 10,000 to 30,000, the relative variations of the two parameters are about 167% and 732%, respectively. In addition, from the definitions of Nu and f (see Eqs. (12) and (13)), one can see that Nu is in proportion to h, and thus rises with an increasing Re or a decreasing L_b. f, proportional to β and inversely proportional to the square of velocity. For the quick reference, double vertical coordinate systems are adopted in Fig. 6, and the data of Nu and f are presented by the right vertical axes of Fig. 6(a) and (b), respectively.

The variation of overall thermo-hydraulic performance, i.e., h/β, is presented in Fig. 6(c). It is clearly seen that h/β lies in the range between 821 and 3991 W/(m^2 K kPa), and it rises with the increment of L_b and the decrement of Re number. In more details, when L_b is increased from 120 to 240 mm, the overall thermo-hydraulic performance rises by about 56% at Re = 20,000.

4.2.2. Effects of rod diameter

Fig. 7(a) and (b) presents the variations of convection heat transfer coefficient (h) and pressure gradient (β) with rod diameter (d) for staggered tubes supported by current rods, respectively, where baffle distance keeps constant of 180 mm and three different Re numbers (i.e., Re = 10,000, 20,000 and 30,000) are computed. It is clearly seen from Fig. 7(a) and (b) that the curves of different Re have similar variation tendencies, and both h and β increase with the increment of d when Re keeps constant. For an instance, when d is increased from 6 to 9 mm at Re = 20,000, h and β rise by 20% and 102%, respectively. In more details, h rises from 6096 to 7310 W/(m^2 K), while β increases from 3160 to 6385 Pa/m. Similar to Figs. 6 and 7(a) and (b) depict the variations of Nu and f with d by the right vertical axes, respectively.

The variation of overall thermo-hydraulic performance (h/β) with rod diameter (d) is depicted in Fig. 7(c). It is observed from Fig. 7(c) that h/β lies in the range between 755 and 3956 W/(m K kPa) for the three Re numbers, and it rises with the decrement of d and Re number. For an instance, when d is decreased from 9 to 6 mm, h/β rises by about 70% at the Re of 20,000.

4.2.3. Effects of clamping methods of tubes

The above investigations in the staggered alignment are all based on the clamping method of one tube within two rods (OTWTR), while the following is to study the clamping method of one tube by one rod (OTBOR), and comparison between the two methods is to be conducted.

Fig. 8(a) presents the variations of convection heat transfer coefficient, h, with Re number for the clamping methods of OTWTR and OTBOR, while their variations of pressure gradient (β) are depicted in Fig. 8(b). Similar to the above treatment, the variations of Nu and f with d are presented by the right vertical axes for quick references, respectively. It is noted that rod diameters (d) keep constant of 7 mm, while baffle distances (L_b) take two values of 150 and 210 mm. It is seen from Fig. 8(a) and (b) that the two types of clamping methods have similar variation tendencies of h (Nu) and β (f), i.e., h (Nu) and β (f) both rise with the increment of Re and the decrement of L_b. Moreover, it is found that compared with OTWTR, OTBOR generates a smaller h and β under the identical Re number, and the decrease of β is more remarkable. For an instance, when Re = 20,000, OTBOR has an h about 82% times that of OTWTR, while its β is decreased by about 57% compared with OTWTR.

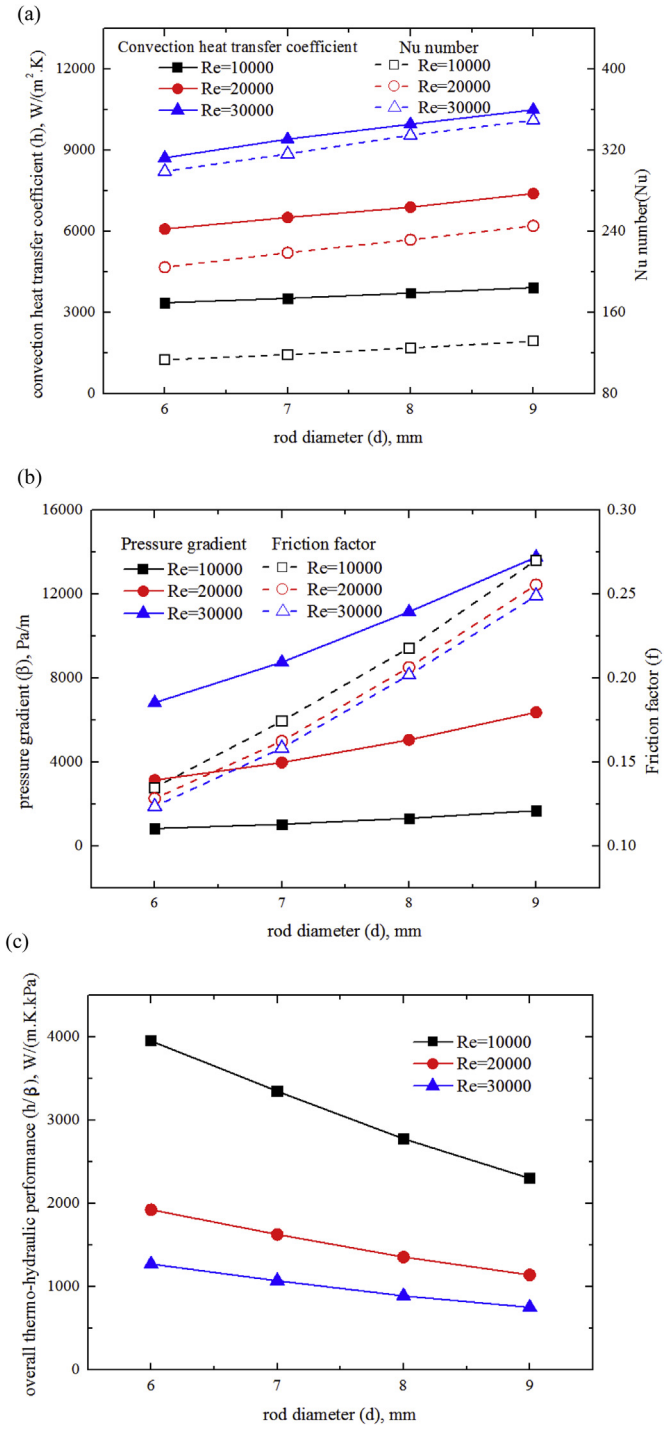

Fig. 7. Variations of thermo-hydraulic performances with rod diameter under different Re conditions. Tubes are clamped with the method of one tube within two rod (OTWTR). (a) Variations of convection heat transfer coefficient and Nu number; (b) variations of pressure loss and friction factor; (c) variation of overall thermo-hydraulic performance.

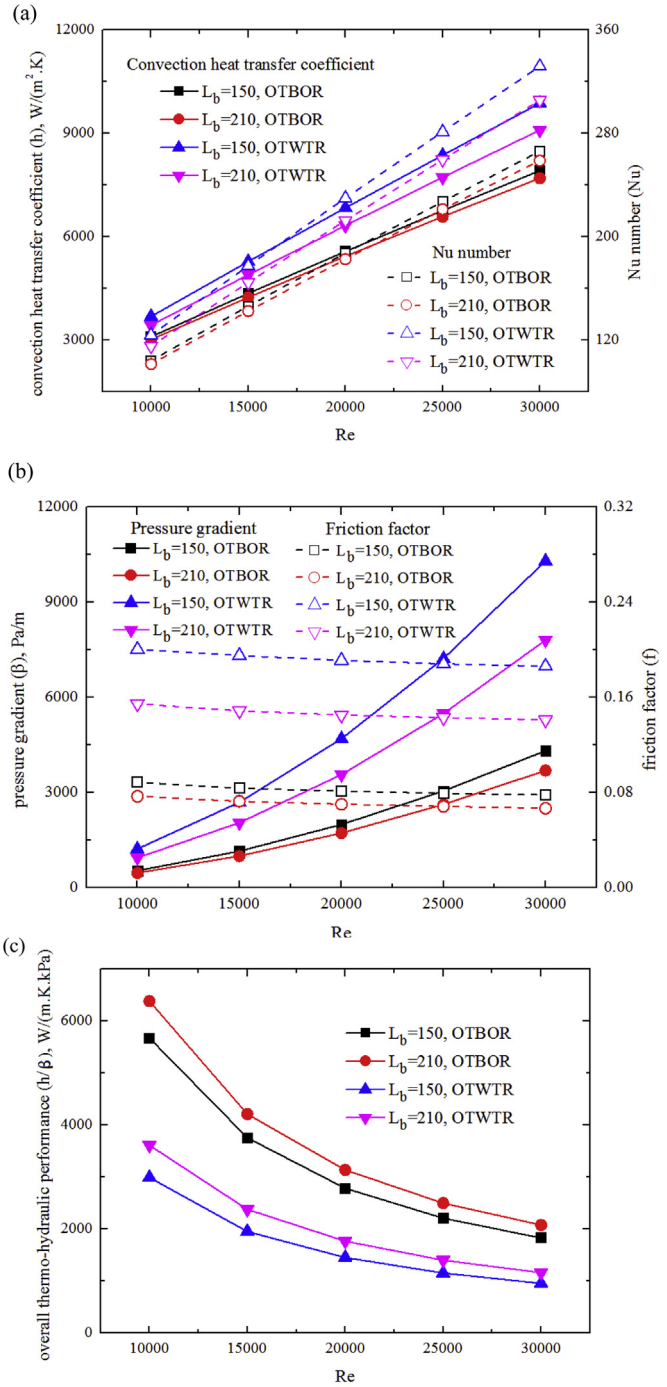

Fig. 8. Comparisons of thermo-hydraulic performances of staggered tubes between clamping methods of one tube by one rod (OTBOR) and one tube within two rods (OTWTR). (a) Comparisons of convection heat transfer coefficient and Nu number; (b) comparisons of pressure loss and friction factor; (c) comparison of overall thermo-hydraulic performance.

The comparison of overall thermo-hydraulic performance, h/β, between OTWTR and OTBOR is presented in Fig. 8(c). One can clearly see from Fig. 8(c) that OTBOR generates a better overall thermo-hydraulic performance. In more details, h/β of OTBOR lies in the range between 926 and 6245 W/(m K kPa), about 91% and 78% higher than the counterparts of OTWTR for the cases of $L_b = 150$ and 210 mm, respectively.

Compared with the counterparts of non-staggered alignment (see Fig. 5), one can see that the convection heat transfer coefficient generated by staggered alignment of OTBOR is increased by about 12% for the case of $L_b = 150$ mm, while its pressure loss is decreased by about 13.5%, resulting in an increment of 30% of overall thermo-hydraulic performance. The relative increment of convection heat transfer coefficient is relatively larger (about 17.8%) when baffle distance $L_b = 210$ mm, while its pressure loss is slightly increased compared with that of non-staggered alignment, and h/β of OTBOR is increased by about 14% for the case of $L_b = 210$ mm.

It is clear that OTBOR has some advantage of overall thermo-hydraulic performance. However, it is noted that staggered alignment of OTBOR has the span between corresponding clamping points two times that of OTWTR, which implies that the alignment of OTBOR could have a larger tube deformation, and thus not facilitate a low vibration level.

5. Analyses and discussions

5.1. Physical mechanism of heat transfer enhancement

The current numerical results demonstrate that the staggered tubes supported by the proposed round rods have a good heat transfer performance. To analyze the physical mechanism, the fluid streamtraces, together with the contours of velocity, temperature, pressure and convection heat transfer coefficient at Re = 20,000,

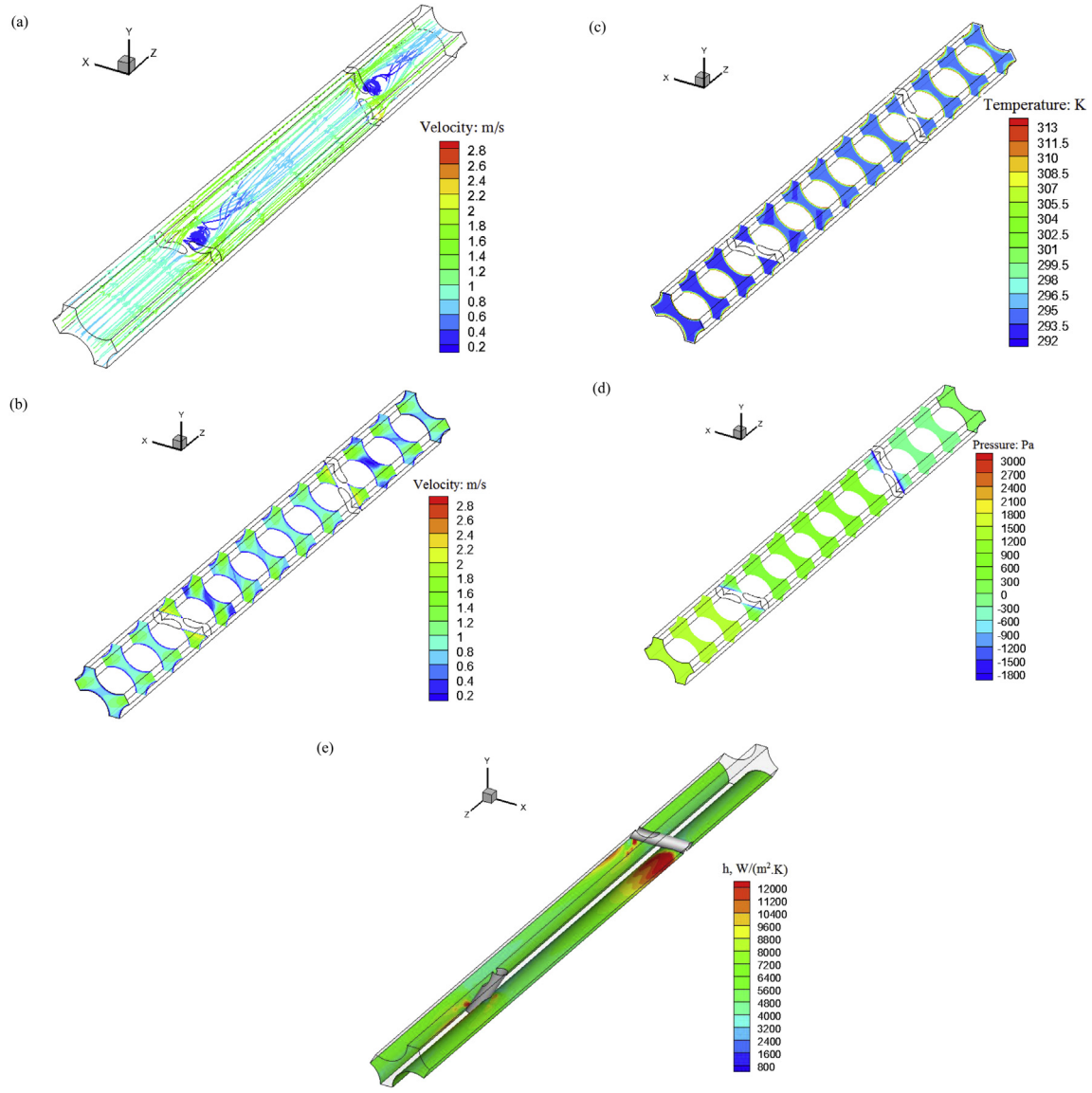

Fig. 9. Fluid streamtraces and contours of velocity, temperature, pressure and convection heat transfer coefficient at Re = 20,000. Rod diameter $d = 7$ mm; Baffle distance $L_b = 180$ mm. Tubes are clamped with the method of one tube within two rods (OTWTR). (a) Streamtraces of fluid flowing longitudinally between staggered tubes; (b) contour of velocity at slices with a constant distance of 1/6 times baffle distance; (c) contour of temperature at slices with a constant distance of 1/6 times baffle distance; (d) contour of pressure at slices with a constant distance of 1/6 times baffle distance; (e) contour of convection heat transfer coefficient of tube walls.

are respectively presented in Fig. 9(a)–(e) for discussion, where rod diameter $d = 7$ mm and baffle distance $L_b = 180$ mm.

From Fig. 9(a) (fluid streamtrace) the acceleration and expansion of working fluid are clearly seen when it flows cross rods, and the flow direction varies periodically, which generates multi-direction jet and spiral flows. Fig. 9(b) presents the velocity contour at different cross sections, where the jet flows induced by rods are also observed. The multi-directional jet and spiral flow flushes downstream tube walls, resulting in an effective heat transfer enhancement, in accordance with the large red regions showed in Fig. 9(e) (contour of convection heat transfer coefficient). Meanwhile, it is observed from Fig. 9(a) and (b) that the recirculation zones induced by the round rods are relatively small, and thus the heat transfer rate is enhanced relatively evenly, in accordance with the shade pattern of Fig. 9(e).

Fig. 9(c) depicts the temperature contour of shellside fluid, where inlet and tube wall temperature are equal to 293 and 313 K, respectively. In Fig. 9(c), a remarkable temperature variation of working fluid is seen between the inlet and outlet, indicating that current Rodbaffles reinforce the heat transfer rate effectively.

Studying the pressure contour, i.e., Fig. 9(d), one can see that the pressure loss of the current Rodbaffle heat exchanger is relatively small, and the majority comes from the flow resistances across rods.

In brief, the staggered tubes supported by current rods have a large convection heat transfer coefficient and a small pressure loss, thus their overall thermo-hydraulic performance is good.

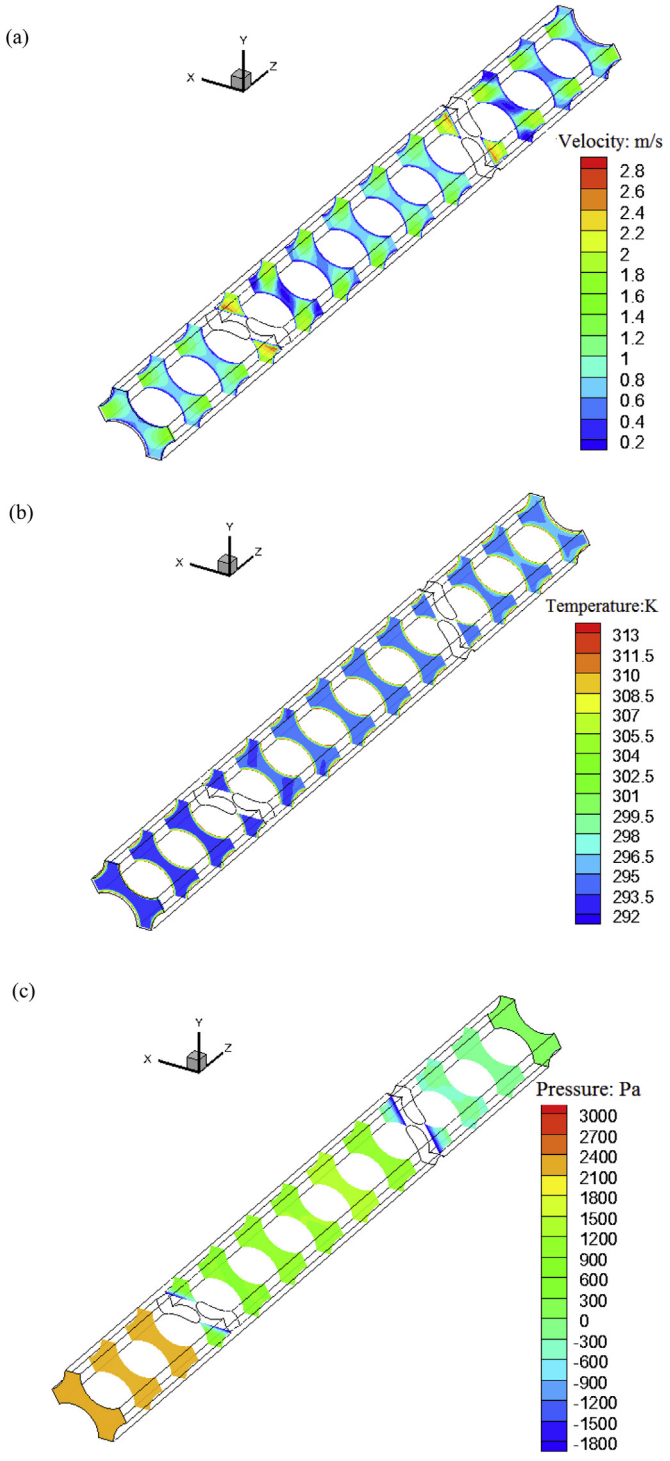

Fig. 10. Contours of velocity, temperature and pressure at Re = 20000. Rod diameter $d = 9$ mm; baffle distance $L_b = 180$ mm. Tubes are clamped with the method of one tube within two rods (OTWTR). (a) Contour of velocity at slices with a constant distance of 1/6 times baffle distance; (b) contour of temperature at slices with a constant distance of 1/6 times baffle distance; (c) contour of pressure at slices with a constant distance of 1/6 times baffle distance.

5.2. *Influences of geometrical factors on thermo-hydraulic performance*

To interpret the variation tendencies of thermo-hydraulic performances with rod diameter (see Fig. 7), the contours of velocity, temperature and pressure of the case with rod diameter $d = 9$ mm and baffle distance $L_b = 180$ mm are presented in Fig. 10(a)–(c), respectively, and compared with the counterparts of the case of $d = 7$ mm and $L_b = 180$ mm (see Fig. 9(b)–(d)). Meanwhile, the contours of velocity, temperature and pressure of the case of $d = 7$ mm and $L_b = 150$ mm are presented in Fig. 11(a)–(c), respectively. They are compared with the counterparts in Fig. 9 to discuss the influences of baffle distance (see Fig. 6). With the comparison of velocity contours (see Figs. 9(b), 10(a) and 11(a)), it is seen that the velocity magnitude of jet flow increases with a rising rod diameter and a decreasing baffle distance. As the jet flow plays a significant role in the heat transfer enhancement and flow resistance, it can be predicted that better heat transfer rate and larger pressure drop are to be obtained by using a larger rod and small baffle distance.

Comparing the temperature contours (see Figs. 9(c), 10(b) and 11(b)), where inlet and tube wall temperatures keep constant (i.e., 293 and 313 K, respectively), it is observed that both Figs. 10(b) and 11(b) have a larger outlet temperature. It indicates that a larger rod and a small baffle distance could generate a higher heat transfer rate, in accordance with the curves in Figs. 7(a) and 6(a).

Studying the pressure contours (see Figs. 9(d), 10(c) and 11(c)), where outlet pressures are equal to zero, one can see that both larger rod diameter and smaller baffle distance lead to a larger pressure loss from the shade at the inlet, in accordance with the curves of Figs. 7(b) and 6(b) as well.

The above discussions are all based on the clamping method of one tube within two rods (OTWTR). To discuss the influences of clamping methods of tubes, the contours of velocity, temperature and pressure of one tube by one rod (OTBOR) are presented in Fig. 12(a)–(c), respectively, where rod diameter d, baffle distance L_b and Re number are identical to the counterparts of OTWTR of Fig. 11.

From the comparison of the velocity contours between OTWTR and OTBOR (see Figs. 11(a) and 12(a)), it is seen that OTBOR has a jet flow with a smaller velocity, and its intensity of spiral flow is relatively weaker, which go against the heat transfer enhancement, while facilitate a smaller flow resistance.

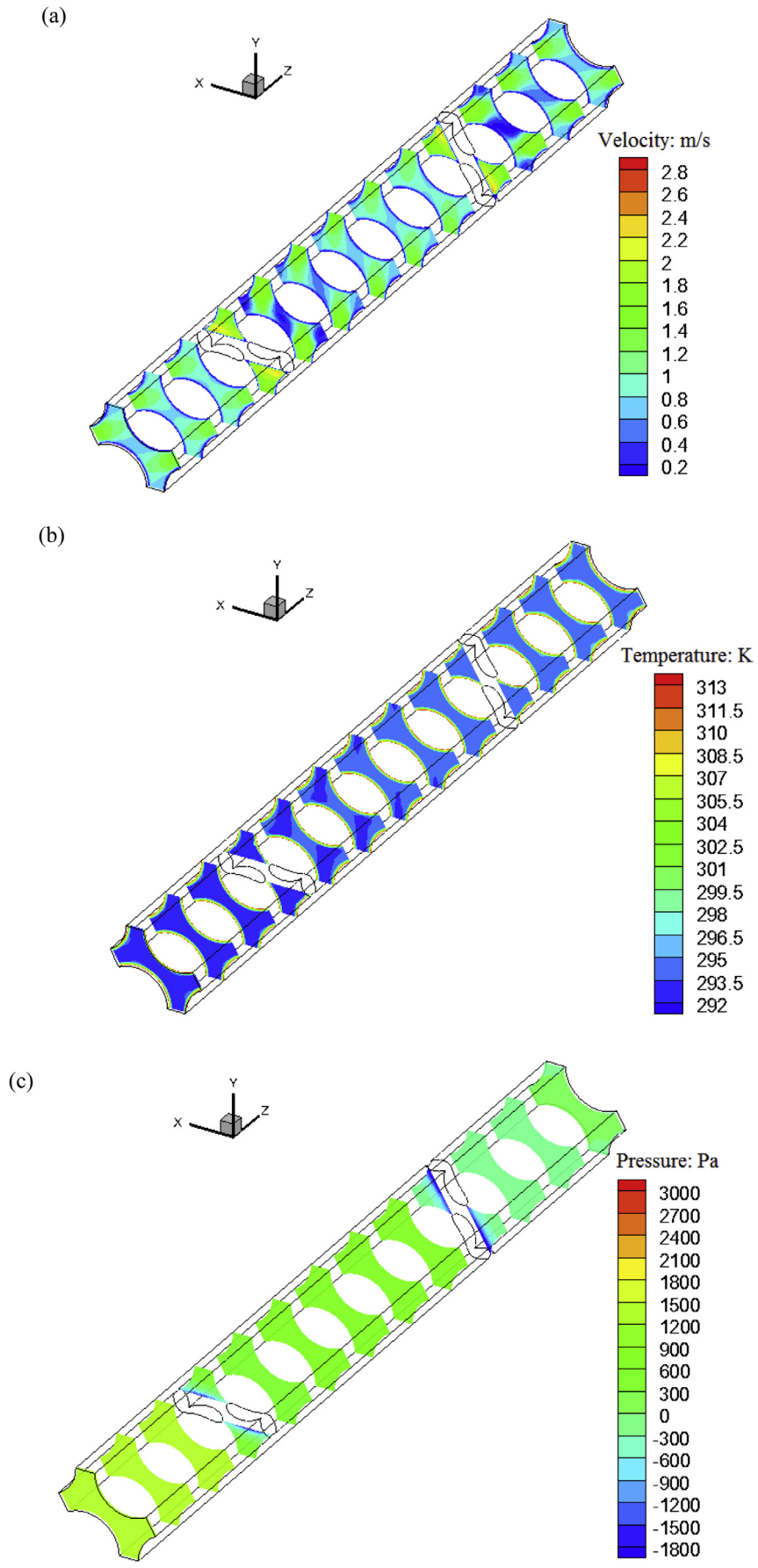

Fig. 11. Contours of velocity, temperature and pressure at Re = 20000. Rod diameter $d = 7$ mm; Baffle distance $L_b = 150$ mm. Tubes are clamped with the method of one tube within two rods (OTWTR). (a) Contour of velocity at slices with a constant distance of 1/6 times baffle distance; (b) contour of temperature at slices with a constant distance of 1/6 times baffle distance; (c) contour of pressure at slices with a constant distance of 1/6 times baffle distance.

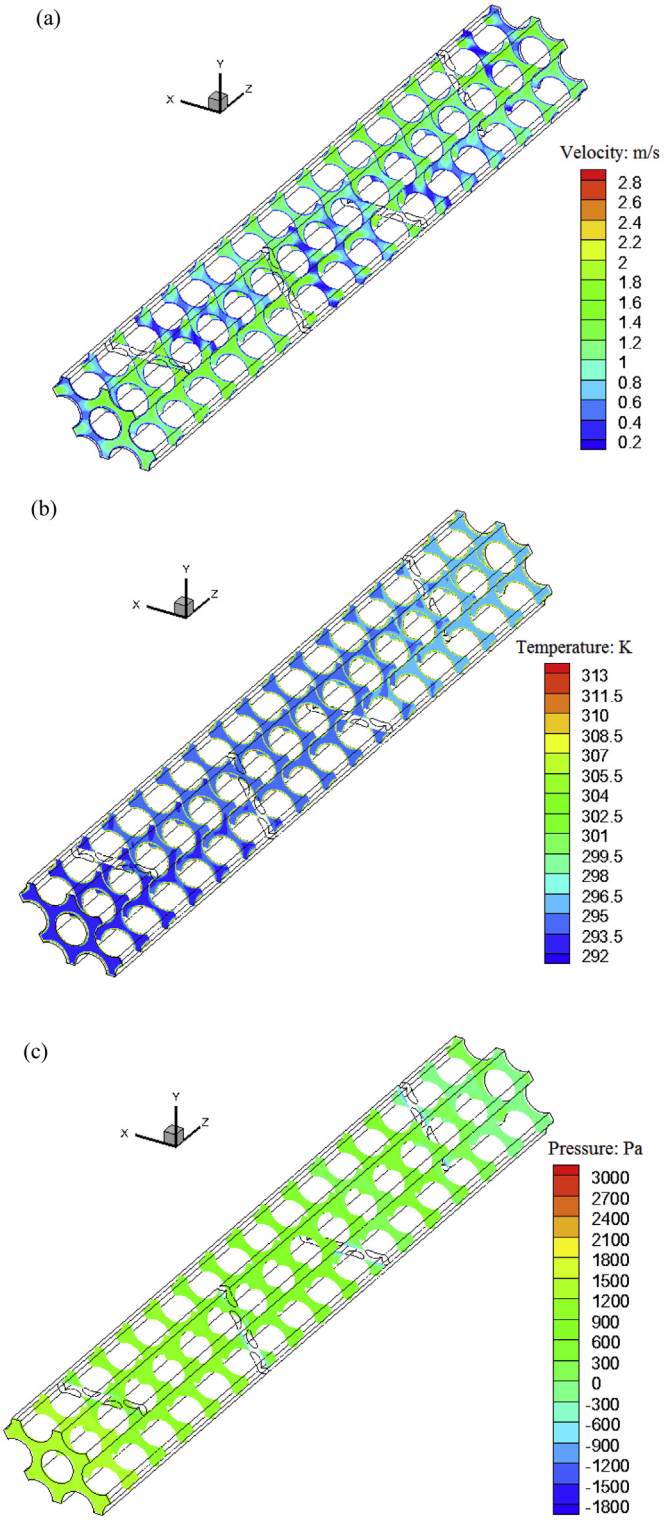

Fig. 12. Contours of velocity, temperature and pressure at Re = 20000. Rod diameter d = 7 mm; Baffle distance L_b = 150 mm. Tubes are clamped with the method of one tube by one rod (OTBOR). (a) Contour of velocity at slices with a constant distance of 1/4 times baffle distance; (b) contour of temperature at slices with a constant distance of 1/4 times baffle distance; (c) contour of temperature at slices with a constant distance of 1/4 times baffle distance.

Comparing the temperature contours of the two clamping methods (see Figs. 11(b) and 12(b)), where the inlet and tube wall temperature are identical, one can observe that the fluid temperature variation of OTBOR is smaller over the same longitudinal displacements, which indicates that the heat transfer rate is better enhanced with OTWTR, in accordance with the curves in Fig. 8(a).

Studying the pressure contours (see Figs. 11(c) and 12(c)), it is clearly seen that OTBOR can induces a much smaller pressure drop over the same longitudinal displacements, and thus generates a better overall thermo-hydraulic performance, in accordance with the curves in Fig. 8(b) and (c).

6. Conclusions

To improve the thermo-hydraulic performance of Rodbaffle heat exchangers, round rods with arc cuts are proposed to be welded with rings to support staggered tubes in the current investigation, and numerical computation is conducted for the turbulent heat transfer enhancement with the current supports. Comparisons of thermo-hydraulic performances between staggered and non-staggered alignments are performed. Meanwhile, the influences of baffle distance (L_b), rod diameter (d) and clamping method of tubes are investigated.

Computation results demonstrate that the convection heat transfer coefficient (h) and combined parameter (hA) of staggered tubes clamped with the method of one tube within two rods (OTWTR) are about 41.9% and 63.8% larger than the counterparts of non-staggered ones, respectively, while the pressure loss is almost doubled. Besides, it is found that h of staggered alignment, ranging between 2835 and 10825 W/(m^2 K), increases with the decrement of L_b and the increment of d, and the pressure loss (β) has a similar variation tendency. The overall thermo-hydraulic performance (h/β) of staggered alignment lies in the range of 821–6243 W/(m K kPa), and a larger L_b, or a smaller d or Re number facilitates a larger h/β. Moreover, it is discovered that the clamping method of one tube by one rod generates a much smaller β and thus a larger h/β compared with the counterparts of OTWTR or non-staggered alignment, however, the former might be unfavorable for a low vibration level. In addition, analyses and discussions are performed based on the fluid streamtraces and contours of velocity, pressure and temperature. The round rods with arc cuts are easy to manufacture, therefore, the proposed tube supports are promising to be used in industrial fields.

Acknowledgements

This work was supported by the National Key Basic Research Development Program of China (2013CB228302).

References

[1] D. Butterworth, Developments in shell-and-tube exchangers, in: ICHMT Int. Symp. on New Developments in Heat Exchangers Lisbon, Portugal, 1993. Paper L.7.
[2] P. Stehlik, V.V. Wadekar, Different strategies to improve industrial heat exchange, Heat Transfer Eng. 23 (6) (2002) 36–48.
[3] A.E. Bergles, ExHFT for fourth generation heat transfer technology, Exp. Therm. Fluid Sci. 26 (2–4) (2002) 335–344.
[4] Y.H. You, A.W. Fan, W. Liu, S.Y. Huang, Thermo-hydraulic characteristics of laminar flow in an enhanced tube with conical strip inserts, Int. J. Therm. Sci. 61 (2012) 28–37.
[5] A.W. Fan, J.J. Deng, A. Nakayama, W. Liu, Parametric study on turbulent heat transfer and flow characteristics in a circular tube fitted with louvered strip inserts, Int. J. Heat Mass Transfer 55 (2012) 5205–5213.
[6] S.J. Green, G. Hetsroni, PWR steam generators, Int. J. Multiphase Flow 21 (1995) 1–97.
[7] Y.H. You, A.W. Fan, X.J. Lai, W. Liu, S.Y. Huang, Experimental and numerical study of thermal-hydraulic performance of a shell-and-tube heat exchanger with trefoil-hole baffles, Appl. Therm. Eng. 50 (1) (2013) 950–956.

[8] J. Lutcha, J. Nemcansky, Performance improvement of tubular heat exchangers by helical baffles, Trans. IChME 68 (A) (1990) 263–270.
[9] D. Kral, P. Stehlik, H.J. Van Der Ploeg, Bashir I. Master, Helical baffles in shell-and-tube heat exchangers, part I: experimental verification, Heat Transfer Eng. 17 (1) (1996) 93–101.
[10] J.F. Zhang, Y.L. He, W.Q. Tao, 3D numerical simulation on shell-and-tube heat exchangers with middle-overlapped helical baffles and continuous baffles-part II: simulation results of periodic model and comparison between continuous and noncontinuous helical baffles, Int. J. Heat Mass Transfer 52 (2009) 5381–5389.
[11] X. Deng, S. Deng, Investigation of heat transfer enhancement of roughened tube bundles supported by ring or rod supports, Heat Transfer Eng. 19 (2) (1998) 21–27.
[12] Y.S. Wang, Z.C. Liu, S.Y. Huang, W. Liu, W.W. Li, Experimental investigation of shell-and-tube heat exchanger with a new type of baffles, Heat Mass Transfer 47 (2011) 833–839.
[13] Y.H. You, A.W. Fan, S.Y. Huang, W. Liu, Numerical modeling and experimental validation of heat transfer and flow resistance on the shell side of a shell-and-tube heat exchanger with flower baffles, Int. J. Heat Mass Transfer 25–26 (55) (2012) 7561–7569.
[14] C.C. Gentry, Rodbaffle heat exchanger technology, Chem. Eng. Prog. 86 (7) (1990) 48–56.
[15] Q.W. Dong, M.S. Liu, Heat Exchanger with Longitudinal Flow of Shellside Fluid, first ed., Chemical Industry Press, Beijing, 2007 (in Chinese).
[16] C.C. Gentry, M.C. Gentry, G.E. Scanlon, Shell and Tube Heat Exchanger Applications, Heating Process and Fluid Flow-PTQ 4, 1999, pp. 95–101.
[17] Q.W. Dong, Y.Q. Wang, M.S. Liu, Numerical and experimental investigation of shellside characteristics for Rodbaffle heat exchanger, Appl. Therm. Eng. 28 (2008) 651–660.
[18] L. Ma, Y.S. Wang, J. Yang, Z.C. Liu, W. Liu, Numerical simulation of rod baffle heat exchangers and its optimum design, J. Eng. Thermophys. 33 (2011) 462–464.
[19] W. Liu, Z.C. Liu, Y.S. Wang, S.Y. Huang, Flow mechanism and heat transfer enhancement in longitudinal-flow tube bundle of shell-and-tube heat exchanger, Sci. China Ser. E Technol. Sci. 52 (10) (2009) 2952–2959.
[20] Q.W. Dong, J. Li, M.S. Liu, Q. Liu, Numerical analysis of heat transfer coefficient of different diameter thermo-tube and disposal mode, Nucl. Power Eng. 27 (2006) 14–17 (in Chinese).
[21] L.W. Yan, J.X. Wu, Z.W. Wang, Industrially experimental investigations and development of the curve-ROD baffle heat exchanger, J. Shanghai Univ. (Engl. Ed.) 8 (3) (2004) 337–341.
[22] Q. Xiong, B. Li, J. Xu, GPU-accelerated adaptive particle splitting and merging in SPH, Comput. Phys. Commun. 184 (2013) 1701–1707.
[23] Q. Xiong, L. Deng, W. Wang, et al., SPH method for two-fluid modeling of particle-fluid fluidization, Chem. Eng. Sci. 66 (2011) 1859–1865.
[24] W.Q. Tao, Numerical Heat Transfer, second ed., Xi'an Jiaotong University Press, Xi' an, 2001 (in Chinese).
[25] J.P. Holman, Heat Transfer, tenth ed., McGraw-Hill, New York, 2002.